HHS Public Access
Author manuscript
Med Comput Vis (2015). Author manuscript; available in PMC 2017 November 30.

Published in final edited form as:
Med Comput Vis (2015). 2016 ; 9601: 83–92. doi:10.1007/978-3-319-42016-5_8.

Subject-specific Estimation of Missing Cortical Thickness Maps in Developing Infant Brains

Yu Meng[1,2], **Gang Li**[2], **Yaozong Gao**[1,2], **John H. Gilmore**[2], **Weili Lin**[2], and **Dinggang Shen**[2]

[1]Department of Computer Science, University of North Carolina at Chapel Hill, NC, USA

[2]Department of Radiology and BRIC, University of North Carolina at Chapel Hill, NC, USA

Abstract

To accurately chart the dynamic brain developmental trajectories in infants, many longitudinal neuroimaging studies prefer having a complete dataset. Unfortunately, missing data at certain time points are unavoidable in longitudinal datasets. To better use incomplete longitudinal data, we propose a novel method to estimate the subject-specific vertex-wise cortical thickness maps at missing time points, by using a customized regression forest, Dynamically-Assembled Regression Forest (DARF). DARF ensures spatial smoothness of the estimated cortical thickness maps and also the computational efficiency. The proposed method can fully exploit the available information from the subjects both with and without missing scans. Our method has been applied to estimate the missing cortical thickness maps in a longitudinal infant dataset, which includes 31 healthy subjects, with each having up to 5 scans. The experimental results indicate that our method can accurately estimate missing cortical thickness maps, with the average vertex-wise error less than 0.23 mm.

Keywords

Missing data completion; longitudinal cortical thickness; infant brain development

---

1 Introduction

In recent years, longitudinal neuroimaging analysis of early postnatal brain development has received increasing attention [1–5], because this can capture both the subject-specific and population-averaged dynamic developmental trajectories of the cerebral cortex. This will help better understand the relationship between normal structural and functional development of the cerebral cortex [6–9], and will also provide important references for understanding of many neurodevelopmental disorders, which are likely caused by the abnormal early brain development [1, 10]. To accurately chart the dynamic early brain developmental trajectories, many studies prefer using the subjects with complete longitudinal scans. However, in longitudinal studies, as shown in Fig. 2(a), missing data at certain time points are unavoidable due to various reasons, such as subject absence from scheduled scans or poor imaging quality. Directly using incomplete longitudinal data would introduce biases and also reduce precision and power in statistical analysis, while discarding subjects with missing data would cause a terrible waste of potentially useful information and also the considerable cost for data acquisition. Owing to the highly dynamic and nonlinear development of the infant brain, a simple linear interpolation or regression cannot accurately estimate the missing data. Although several other methods have been proposed to estimate or complete the missing data for general purpose [11, 12], their effectiveness reduces with the increase of the portion of missing data. To deal with large portion of missing data, the low rank matrix completion methods have been proposed [13, 14]; however, they work well only if the missing data are distributed randomly and uniformly. Thus, the existing methods are not suitable for estimation of regionally-heterogeneous and longitudinally-dynamic cortical thickness map in infant brain studies.

To bridge this critical gap, in this paper, we unprecedentedly propose a novel general learning-based framework for subject-specific estimation of the vertex-wise *cortical thickness* map at the missing time point(s) in longitudinal infant brain studies. Of note, cortical thickness is an important macroscopic morphological measure of the cerebral cortex in MRI studies, and changes of CT are found in normal development, aging, and brain disorders, indicating differential underlying microstructural changes of the cortex in different states [10]. Technically, we propose a Dynamically-Assembled Regression Forest (DARF), a customized version of random forest, as our core regression tool. By sharing decision trees with neighboring forests, DARF ensures spatial smoothness of the vertex-wise regression/estimation result and also greatly reduces the training time, compared to the conventional regression forest. Hereafter, we refer the vertex-wise cortical thickness maps at missing time points as missing data. To fully exploit the information of both the subjects with complete longitudinal data and the subjects with missing data, our method contains two major stages. In the first stage, to use as many training subjects as possible, the missing data at each time point of each subject is estimated *multiple times* based on the data at different available time points *independently*, and then these estimated results are averaged as the initial estimation. In the second stage, to better capitalize on longitudinal information and make the estimations temporally consistent, the missing data at each time point of each subject is refined based on both the real data and the initially estimated missing data at all the other time points *jointly*. As shown in the experiments, our method can accurately estimate the subject-specific cortical thickness map at missing time points in longitudinal infant studies, with the average vertex-wise error less than 0.23 mm.

2 Methods

In this section, we first introduce our regression model, namely Dynamically-Assembled Random Forest (DARF), and then describe how to use this regression model for subject-specific estimation of vertex-wise cortical thickness map at the missing time point(s) in longitudinal infant studies. Of note, before the estimation of missing data, the longitudinal cortical surfaces of all infants were reconstructed [15] and warped onto the same *spherical* space to establish both intra-subject and inter-subject cortical correspondences, and subsequently all cortical surfaces were resampled to have the same triangular mesh configuration using a method similar to [16]. Cortical thickness and sulcal depth were computed for each vertex on each cortical surface [15, 16].

2.1 Dynamically-Assembled Regression Forest

Motivation—We adopt regression forest [17] as our core regression tool. However, using only one conventional regression forest (CRF) cannot accurately estimate vertex-wise cortical thickness maps, because cortical thickness and its developmental patterns are both regionally heterogeneous. An intuitive way to solve this issue is to first divide the cortical surface into a set of small regions of interest (ROIs), and then train a specific regression forest for each ROI. However, this will lead to spatially unsmooth estimation results around the boundaries of neighboring ROIs, since the cortical thicknesses of the vertices near to the ROI boundary are estimated using two completely different regression forests, which are trained independently with different training samples. Although using the highly overlapped ROIs could produce relatively smooth estimation results, it requires a large set of ROIs to uniformly cover the whole cortex, and thus leads to large computational workload. To address these issues, we proposed a Dynamically-Assembled Regression Forest (DARF). By sharing large portions of trees with the neighboring forests, DARF can make the estimation result as smooth as the real data, and also greatly reduce the training time.

Training & Testing—In the training stage, an individual binary decision tree is trained at each vertex on the spherical surface. Specifically, as shown in Fig. 1(a), for a given vertex, all its nearby vertices in a specified neighborhood (i.e., red region) on the spherical cortical surface are used as training samples. For each training sample i, we have a feature vector $\boldsymbol{X}_i \in \mathbb{R}^d$ and a regression response $y_i \in \mathbb{R}$. The feature vector $\boldsymbol{X}_i$ consists of a set of features (see Section 2.2) extracted from the local cortical attribute (e.g., cortical thickness and sulcal depth) maps at input time points, and the regression response y_i is the cortical thickness value at the target time point. In the testing stage, to estimate the cortical thickness at a given vertex, as shown in Fig. 1(b), all the nearby individual trees trained for vertices in a specified neighborhood (i.e., green region) are grouped together to form a DARF. Then the feature vector of the given vertex is fed to the DARF to estimate the cortical thickness at the target time point.

Smoothness—DARF is able to produce spatially very smooth estimations, because 1) the DARFs of neighboring vertices are very similar, as they share a large number of trees, and 2) the features of neighboring vertices are also similar.

2.2 Feature Computation on Spherical Surface

For each vertex i, its feature vector $\boldsymbol{X_i} \in \mathbb{R}^d$ includes two types of features: local features and context features. Herein, local features provide localized information at each vertex, while context features provide rich neighboring information. In our implementation, local features are the cortical thickness and sulcal depth. The context features are a set of randomly defined Haar-like features, which provide two types of context information: (1) the mean attributes (i.e., cortical thickness and sulcal depth) in a small cortical region, and (2) the difference between mean attributes in two small regions. The computation of Haar-like features on spherical surfaces is shown in Fig. 1(c). Specifically, given a vertex (u_i, v_i), where u_i and v_i are respectively the latitude and longitude coordinates, two blocks A and B are randomly selected in the neighborhood $[u_i \pm u_\theta, v_i \pm v_\theta]$, and their sizes are also randomly chosen from the interval $[r_1, r_2]$, where u_θ, v_θ, r_1, and r_2 are the user-defined parameters. Let

S_a and S_b denote the sets of all the vertices in blocks A and B, respectively, and then the Haar-like features at the vertex (u_i, v_i) can be mathematically formulated as:

$$f(u_i, v_i) = \frac{1}{|S_a|} \sum_{(u,v) \in S_a} M(u, v) - \lambda \frac{1}{|S_b|} \sum_{(u,v) \in S_b} M(u, v) \quad (1)$$

where $M(u,v)$ is the value of cortical morphological attributes (i.e., cortical thickness and sulcal depth) at vertex (u, v), and λ is a random coefficient that can only be 0 or 1. In the case of $\lambda = 0$, Haar-like feature is the mean value of the cortical attribute within the block A. In the case of $\lambda = 1$, Haar-like feature is the difference betweenthe mean values of the cortical attribute in the block A and block B.

2.3 Estimation of Cortical Thickness Maps at Missing Time Points

Fig. 2(a) shows the longitudinal infant dataset with missing data used in this paper, which includes 31 subjects (with 15 subjects having missing data), each subject with up to 5 time points in the first postnatal year. Intuitively, using the data at multiple available time points to estimate the missing ones is better than using the data at just one available time point, because multiple time points capture more information of the nonlinear longitudinal cortex development in infants. However, owing to the missing data, as shown in Fig. 2(a), the more time points we use, the less subjects can be used as training subjects. To fully capitalize on the information of all time points and all subjects, we propose a two-stage method, including (Stage 1) pair-wise estimation between different time points to form a pseudo-complete data, and (Stage 2) joint refinement based on the pseudo-complete data, as shown in Fig. 2(b).

In **Stage 1**, to capitalize on as many training subjects as possible, the cortical thickness map of a subject at each missing time point is estimated using the data at each of other available time points *independently*, and then these independent estimations are averaged together to obtain an initial estimation. For example, to obtain the initial estimation at 6-months-old, we first use the subjects with available data at both 1- and 6-months-old as training subjects to train a set of decision trees, for estimating the data at 6-months-old based on the data at 1-month-old. Then, after training, for the subjects with available data at 1-month-old but without data at 6-months-old, those trained decision trees are locally assembled as forests to estimate the missing data at 6-months-old. Similarly, we can also obtain the estimation of the missing data at 6-months-old, respectively, based on the available data at each of the 3-, 9-, and 12-months-old. In this way, all available data at all other time points can contribute to the estimation of missing data at 6-months-old. Finally, we average all those estimations (contributed from different time points) as the initial estimation. Similarly, for the missing data at 1-, 3-, 9-, and 12-months-old, the same process can be performed to obtain their initial estimations. After **Stage 1**, all the missing data of all subjects will be approximately recovered, thus providing a pseudo-complete longitudinal dataset.

In **Stage 2**, to take advantage of the longitudinal information and also to make the estimation temporally consistent, the missing data at each time point of each subject is further refined using all the data at all other time points *jointly*. For example, to obtain the final estimation of the missing data at 6-months-old, we use all the subjects that have *real* data at 6-months-old as training subjects to train a set of decision trees, which can estimate the missing data at 6-months-old based on the given data at 1-, 3-, 9-, and 12-months-old jointly. Note that we do not require each training/testing subject to have *real* data at 1-, 3-, 9-, and 12-months-old. If a training/testing subject has missing data at 1-, 3-, 9-, or 12-months-old, its initial estimation that has been estimated in **Stage 1** can be used. Thus, after training for each subject with missing data at 6-months-old, the trained decision trees can be locally assembled as forests to estimate its missing data. Similarly, for the missing data at other time points, the same process can be conducted to obtain their final estimations. It is worth noting that, using the above two stages, our method leverages information from all time points of all subjects for missing data estimation.

3 Results

The dataset we used in the experiments are illustrated in Fig. 2(a), including 31 healthy infants (with 15 infants having missing data), in which each subject was scheduled to be scanned at 1, 3, 6, 9, and 12 months of age. To evaluate our regression model DARF, we conducted an experiment of using cortical thickness and sulcal depth at one time point to estimate cortical thickness at another time point. The motivation to use sulcal depth for helping estimation of cortical thickness is that these two cortical attributes are highly related [18].

To better demonstrate the effectiveness of DARF, we compared it with other three representative methods, including linear regression (LR), global regression forest (GRF), and sparse linear regression (SLR). LR method learned a linear relationship between cortical thickness at a known time point and cortical thickness at missing time point for each vertex on the cortical surface. GRF method trained a single forest for the entire surface, and used spherical location of each vertex as features, in addition to the Haar-like features. SLR is a popular and effective method for high- dimensional data analysis [19, 20]. By setting the coefficients of irrelevant feature elements as zero, SLR is able to extract the most useful features from a highdimensional feature representation, making it a reasonable competitor of DARF. Specifically, given the target vector $\mathbf{Y}=[y_1, y_2, \ldots, y_n]^T \in \mathbb{R}^n$ and the feature matrix $\mathbf{X}=[\boldsymbol{X}_1, \boldsymbol{X}_2, \ldots, \boldsymbol{X}_n] \in \mathbb{R}^{d \times n}$, SLR method finds the optimal coefficients $\mathbf{A} = [a_1, a_2, \ldots, a_d]^T \in \mathbb{R}^d$ by solving Eq. 2 below, with the constraint that the number of non-zero elements in $\mathbf{A}$ is no more than L.

$$\underset{\alpha \in \mathbb{R}}{argmin} \frac{1}{2} \| \boldsymbol{Y} - \boldsymbol{X}^T \boldsymbol{A} \|_2^2 + \lambda \| \boldsymbol{\alpha} \|_1 \quad (2)$$

To make the comparison fair, we used the same training data with the same features for both SLR and DARF, and we also optimally set L=12 and, λ=0.001 based on a grid search, which was performed on a subset of the training data.

To quantitatively evaluate the estimation results, we employed two metrics: mean absolute error ($MAE = |\boldsymbol{T}_e - T_t|/N$) and mean relative error ($MRE = |(\boldsymbol{T}_e - \boldsymbol{T}_t)/\boldsymbol{T}_t|/N$), where T_t and T_e are respectively the ground-truth and estimated values of cortical thickness, and N is the number of vertices. Fig. 3 provides a comparison of LR, GRF, SLR, and DARF for estimation of vertex-wise cortical thickness map at 9 months of age using cortical attributes at 1 month of age on a representative subject. As we can see, DARF estimated more accurate cortical thickness maps than all the other methods, especially in some highlighted challenging regions, such as the frontal pole, rostral middle frontal gyrus, and supramarginal gyrus. For comprehensive comparisons, we repetitively estimated the cortical thickness maps at 3-, 6-, 9-, and 12 months of age using the data at 1 month of age for all the available subjects, and performed a leave-one-out cross validation for each target time point. As reported in Table 1. Hence, we can conclude that DARF performs significantly better than the other three methods in estimating vertex-wise cortical thickness maps.

To evaluate the proposed missing data estimation method, we tested our method by recovering the data of cortical thickness at 5 missing time points. Specifically, from our longitudinal dataset (Fig. 2a), we randomly selected 5 subjects that had complete data at all 5 time points as the reference subjects. For each of these reference subjects, we manually deleted the data at one time point, and then put it back to the dataset. We run our missing data estimation method to recover the missing data, and then compared it with the ground truth. This experiment was repeated 12 times, with each time using 5 different subjects as reference subjects. We also performed paired t-test to statistically compare the results of pairwise estimation (Stage 1) and joint refinement (Stage 2). Fig. 4 shows the results of our method for estimation of cortical thickness at 1, 3, 6, 9, and 12 months of age on a typical infant. The complete quantitative evaluation is reported in Table 2, from which we can conclude that: (1) our method can effectively estimate the missing cortical thickness maps with the average error less than 0.23 mm; and (2) joint refinement significantly improves the results of pairwise estimation. Note that among all time points the estimations were relatively less accurate at around 6 months of age, due to the extremely low image contrast and exceptionally rapid cortex development during this stage [15]. Of note, Table 2 shows better results than Table 1, because only the 1-month-old data was used for estimation in Table 1, while all available time-point data was used in Table 2. We further reported the estimation errors in 35 cortical ROIs, as shown in Fig. 5. We can see that in all ROIs, the joint refinement clearly improves the results, with particularly large improvement in the cingulate cortex, cuneus cortex, orbitofrontal cortex, middle temporal gyrus, pars orbitalis, pericalcarine cortex, and superior frontal gyrus.

4 Conclusion

This paper has two major contributions. First, we proposed DARF to ensure the spatial smoothness of regression results and also the computational efficacy, by sharing decision trees with neighboring forests. Second, we proposed a two-stage method to unprecedentedly estimate subject-specific vertex-wise cortical thickness maps at the missing time point(s) in longitudinal infant study, by fully exploiting the available information from all subjects. Of note, our method is very generic and not limited to estimate only cortical thickness, as it can be extended to estimate other cortical anatomical attributes, such as surface area, sulcal depth, and local cortical gyrification [21].

References

1. Gilmore JH, Shi F, Woolson SL, Knickmeyer RC, Short SJ, Lin W, Zhu H, Hamer RM, Styner M, Shen D. Longitudinal development of cortical and subcortical gray matter from birth to 2 years. Cerebral cortex. 2012; 22:2478–2485. [PubMed: 22109543]
2. Li G, Nie J, Wang L, Shi F, Lin W, Gilmore JH, Shen D. Mapping region-specific longitudinal cortical surface expansion from birth to 2 years of age. Cerebral cortex. 2013; 23:2724–2733. [PubMed: 22923087]
3. Li G, Nie J, Wang L, Shi F, Lyall AE, Lin W, Gilmore JH, Shen D. Mapping longitudinal hemispheric structural asymmetries of the human cerebral cortex from birth to 2 years of age. Cerebral cortex. 2014; 24:1289–1300. [PubMed: 23307634]
4. Meng Y, Li G, Lin W, Gilmore JH, Shen D. Spatial distribution and longitudinal development of deep cortical sulcal landmarks in infants. NeuroImage. 2014; 100:206–218. [PubMed: 24945660]
5. Nie J, Li G, Wang L, Shi F, Lin W, Gilmore JH, Shen D. Longitudinal development of cortical thickness, folding, and fiber density networks in the first 2 years of life. Human brain mapping. 2014; 35:3726–3737. [PubMed: 24375724]
6. Awate SP, Yushkevich PA, Song Z, Licht DJ, Gee JC. Cerebral cortical folding analysis with multivariate modeling and testing: Studies on gender differences and neonatal development. Neuroimage. 2010; 53:450–459. [PubMed: 20630489]
7. Dubois J, Benders M, Borradori-Tolsa C, Cachia A, Lazeyras F, Ha-Vinh Leuchter R, Sizonenko SV, Warfield SK, Mangin JF, Huppi PS. Primary cortical folding in the human newborn: an early marker of later functional development. Brain : a journal of neurology. 2008; 131:2028–2041. [PubMed: 18587151]
8. Gilmore JH, Lin W, Prastawa MW, Looney CB, Vetsa YS, Knickmeyer RC, Evans DD, Smith JK, Hamer RM, Lieberman JA, Gerig G. Regional gray matter growth, sexual dimorphism, and cerebral asymmetry in the neonatal brain. The Journal of neuroscience : the official journal of the Society for Neuroscience. 2007; 27:1255–1260. [PubMed: 17287499]
9. Schnack HG, van Haren NE, Brouwer RM, Evans A, Durston S, Boomsma DI, Kahn RS, Hulshoff Pol HE. Changes in thickness and surface area of the human cortex and their relationship with intelligence. Cerebral cortex. 2015; 25:1608–1617. [PubMed: 24408955]
10. Lyall AE, Shi F, Geng X, Woolson S, Li G, Wang L, Hamer RM, Shen D, Gilmore JH. Dynamic Development of Regional Cortical Thickness and Surface Area in Early Childhood. Cerebral cortex. 2015; 25:2204–2212. [PubMed: 24591525]
11. Troyanskaya O, Cantor M, Sherlock G, Brown P, Hastie T, Tibshirani R, Botstein D, Altman RB. Missing value estimation methods for DNA microarrays. Bioinformatics. 2001; 17:520–525. [PubMed: 11395428]
12. Tsiporkova E, Boeva V. Two-pass imputation algorithm for missing value estimation in gene expression time series. Journal of bioinformatics and computational biology. 2007; 5:1005–1022. [PubMed: 17933008]
13. Candès E, Recht B. Exact Matrix Completion via Convex Optimization. Found Comput Math. 2009; 9:717–772.
14. Liu J, Musialski P, Wonka P, Ye J. Tensor completion for estimating missing values in visual data. IEEE transactions on pattern analysis and machine intelligence. 2013; 35:208–220. [PubMed: 22271823]
15. Li G, Nie J, Wang L, Shi F, Gilmore JH, Lin W, Shen D. Measuring the dynamic longitudinal cortex development in infants by reconstruction of temporally consistent cortical surfaces. Neuroimage. 2014; 90:266–279. [PubMed: 24374075]
16. Li G, Wang L, Shi F, Lin W, Shen D. Constructing 4D infant cortical surface atlases based on dynamic developmental trajectories of the cortex. Medical image computing and computer-assisted intervention. 2014; 17:89–96.
17. Breiman L. Random Forests. Machine Learning. 2001; 45:5–32.
18. Fischl B, Dale AM. Measuring the thickness of the human cerebral cortex from magnetic resonance images. Proceedings of the National Academy of Sciences of the United States of America. 2000; 97:11050–11055. [PubMed: 10984517]

19. Tibshirani R. Regression shrinkage and selection via the Lasso. J Roy Stat Soc B Met. 1996; 58:267–288.
20. Zhang S, Zhan Y, Dewan M, Huang J, Metaxas DN, Zhou XS. Towards robust and effective shape modeling: sparse shape composition. Medical image analysis. 2012; 16:265–277. [PubMed: 21963296]
21. Li G, Wang L, Shi F, Lyall AE, Lin W, Gilmore JH, Shen D. Mapping longitudinal development of local cortical gyrification in infants from birth to 2 years of age. The Journal of neuroscience. 2014; 34:4228–4238. [PubMed: 24647943]

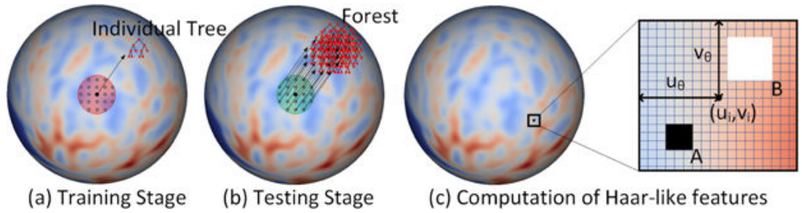

Fig. 1.

Illustration of training and testing stages of DARF, and also the computation of Haar-like features on a spherical surface. In (a), the red region is the neighborhood, where all the vertices are used as training samples. In (b), the green region is the neighborhood, where all trained individual trees are assembled as a forest. Note that the red and green regions can be in different sizes. In (c), the white and black blocks are the two randomly selected regions for computing Haar-like features.

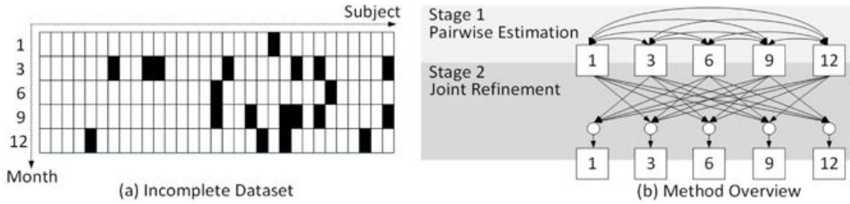

Fig. 2.

Overview of our longitudinal infant dataset and the proposed missing data estimation method. In **(a)**, each column indicates a subject, and each row indicates a time point, where the black blocks indicate the missing data at particular time points. In **(b)**, each box with a time-point number stands for the data at the corresponding time point. The directed edges represent the processes of missing data estimation at the target time points (pointed by the arrowhead) by using the data at the available time points (at the tail side). The bidirectional edges in Stage 1 mean that the estimation is performed bidirectionally by exchanging the input time point and the target time point. The circles in Stage 2 mean using multiple time points *jointly*.

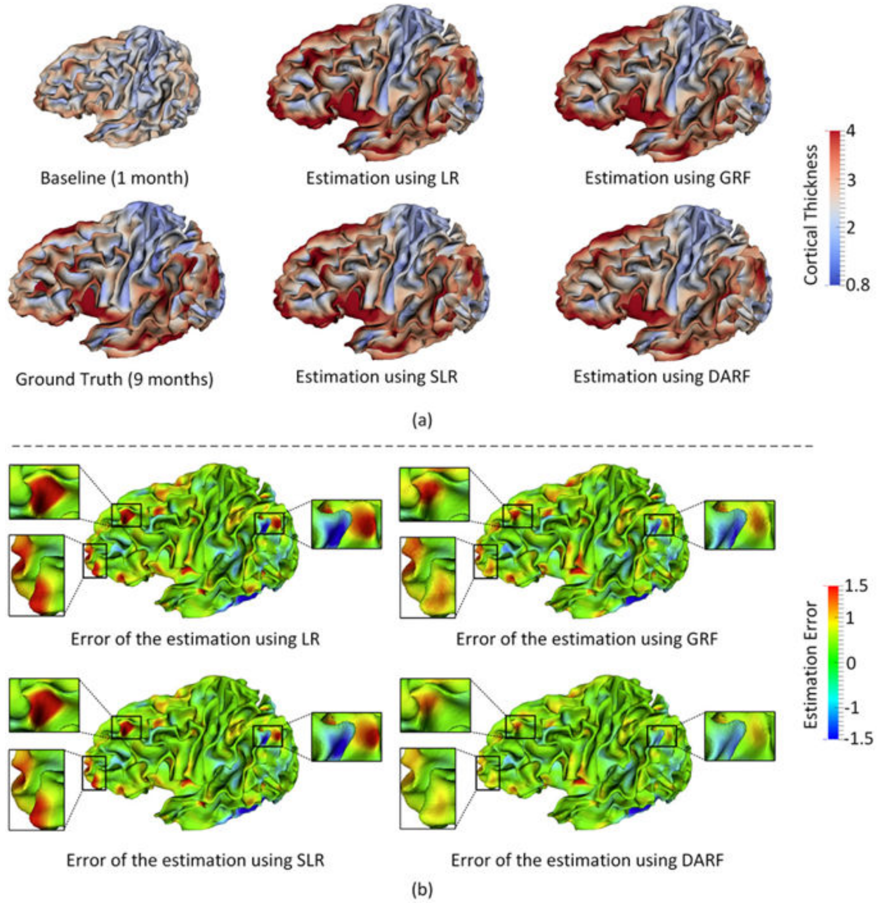

Fig. 3.

Estimation of the cortical thickness map at 9 months of age using the data at 1 month of age for a typical infant. (a) shows the cortical thickness maps in mm at 1 and 9 months of age, and the estimation results using different methods, i.e., LR, GRF, SLR, and DARF. (b) shows the vertex-wise error maps in mm by different methods.

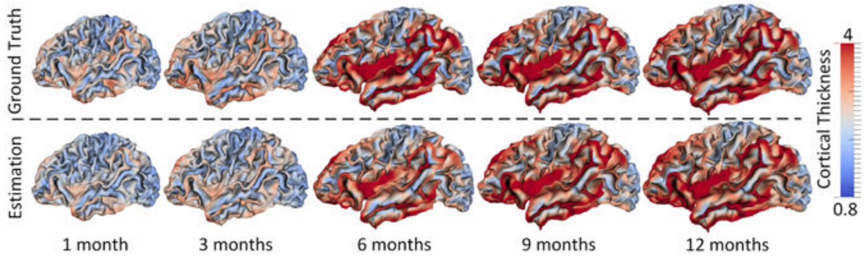

Fig. 4.
Estimation of the missing cortical thickness maps (mm) for a typical infant.

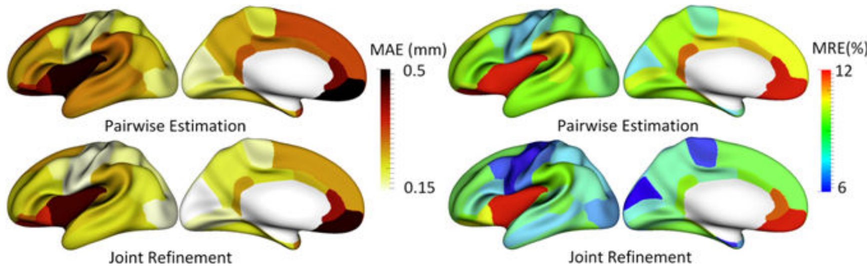

Fig. 5.

Errors of estimation of the missing cortical thickness maps at 9 months of age in 35 ROIs.

Table 1

Quantitative evaluation of the estimation errors of cortical thickness at 3, 6, 9, and 12 months of age, by using different methods, based on the cortical attributes at 1 month of age.

Metric	Methods	3 months	6 months	9 months	12 months
MAE (mm)	LR	0.209±0.033	0.336±0.041	0.342±0.033	0.322±0.028
	GRF	0.209±0.027	0.335±0.039	0340±0.026	0.321±0.025
	SLR	0.207±0.029	0.329±0.040	0.338±0.025	0.320±0.024
	DARF	**0.205±0.027**	**0.316±0.042**	**0.326±0.026**	**0.310±0.026**
	p-value (SLR vs. DARF)	**0.0013**	**3×10^{-13}**	**1×10^{-9}**	**4×10^{-9}**
MRE (%)	LR	10.21±2.03	13.94±1.19	12.95±0.97	12.07±0.72
	GRF	10.17±1.66	13.88±1.21	12.56±0.98	11.87±0.86
	SLR	10.09±1.51	13.12±1.18	12.46±0.97	11.67±0.78
	DARF	**10.00±1.51**	**12.59±1.12**	**12.05±0.93**	**11.30±0.76**
	p-value (SLR vs. DARF)	**0.0032**	**8×10^{-14}**	**1×10^{-10}**	**3×10^{-10}**

Table 2

Quantitative evaluation of estimation results for the missing cortical thickness maps using the proposed method.

Target	MAE (mm)			MRE (%)		
	Stage 1	**Stage 2**	**p-value**	**Stage 1**	**Stage 2**	**p-value**
1 month	0.179±0.015	**0.169±0.013**	**5×10^{-4}**	8.94±0.89	**8.32±0.65**	**3×10^{-4}**
3 months	0.208±0.027	**0.194±0.025**	**8×10^{-6}**	10.01±1.33	**9.24±1.26**	**6×10^{-7}**
6 months	0.252±0.041	**0.233±0.034**	**2×10^{-4}**	9.91±0.72	**9.08±0.77**	**6×10^{-6}**
9 months	0.261±0.021	**0.225±0.016**	**7×10^{-8}**	9.50±0.56	**8.15±0.50**	**2×10^{-9}**
12 months	0.246±0.019	**0.215±0.016**	**7×10^{-11}**	9.04±0.46	**7.82±0.49**	**9×10^{-12}**